Aeroelastic Stability Analysis of a Quad-Rotor Wind Turbine

Etana Ferede [1], Alexander Stillman [2], and Farhan Gandhi [3]
Center for Mobility with Vertical Lift (MOVE)
Rensselaer Polytechnic Institute, Troy, NY, 12180, USA

Abstract. This paper presents the aeroelastic stability analysis of a quad-rotor wind turbine and identifies modes with low damping that are otherwise not present on a single-rotor wind turbine. The non-linear dynamics of a wind turbine model in SIMPACK, without considering wind shear and tower shadow, is linearized around a steady-state; followed by MBC transformation resulting in LTI model. Standard eigenvalue analysis of LTI model is carried out to capture the natural frequency and damping of a quad-rotor wind turbine as a function of wind speed. Results show that several modes with low damping (besides the low damping modes observed on a single-rotor wind turbines) are identified where the damping ratio is less than 1% over the entire operation range.
Keywords: Multi-Rotors Wind Turbine, Eigenvalue analysis, Natural frequency, Damping ratio

1. Introduction

Aeroelastic stability analysis of wind turbines during the design stage is necessary to identify any natural modes with low damping and introduce design modification or devise strategies to ensure adequate damping margins over the operating regime. This becomes increasingly significant as the wind turbines scale up in size for capacity. Consequently, stability analysis of Horizontal Axis Wind Turbines (HAWT) is not new and numerous research papers are available dedicated to the stability analysis of such systems [1-9].

Conversely, few modal analyses of multi-rotor wind turbines are available; among the few, [10] presents a method to analyse the modal dynamics of multi-rotor wind turbines and demonstrates the capability of the method on a three-rotor configuration supported on a single tower; the same authors present a follow up work [11] where the aerodynamic loads are considered in the stability analysis of a tri-rotor wind turbine. Furthermore, [12] presents a modal analysis of a quad-rotor wind turbine. The published work so far on Eigen analyses of multi-rotor wind turbines focuses mainly on evaluating the natural frequency and the associated mode shapes. To the authors' knowledge, there is only one study published that specifically deals with the stability analysis of multi-rotor wind turbines including the aerodynamic loads.

Stability analysis is usually performed by linearizing a non-linear time variant dynamic system around a steady-state point resulting in Linear Time Invariant (LTI) or (in the case of wind turbines) Linear Time Periodic (LTP) system. The equation of motion of wind turbine rotors is in rotating system, which in general are periodic in nature due to wind shear, tower shadow, and/or gravity. First, Multi-Blade Coordinate (MBC) [13] transformation is used to write all the states of a wind turbine in the fixed frame. The periodicity of the system is generally weaker after MBC transformation [4-6]. Thereafter, two approaches can be used to study the stability of the resulting system, namely: (i) the constant coefficient method, where the system matrices are averaged around the azimuth and an eigen-analysis is performed on the resulting LTI system. (ii) direct application of Floquet theory [7,8,9].

This paper builds on the previous work [12] and presents a method for stability analysis of quad-rotor wind turbine. The non-linear model of a 6MW quad-rotor wind turbine is linearized around a quasi-steady point; followed by MBC transformation of the LTP system yielding LTI model. Standard eigenvalue analysis is employed to capture the natural frequency and damping of a quad-rotor wind turbine.

2. Model Description

The quad-rotor wind turbine is modelled using the multi-body simulation (MBS) software SIMAPCK [13] coupled with the NREL aerodynamics software AerodynV15 [14] to calculate the blade aerodynamic loads. SIMPACK is

[1] Research scientist, Mechanical, Aerospace, and Nuclear Engineering, ferede@rpi.edu
[2] Graduate student, Mechanical, Aerospace, and Nuclear Engineering, stilla@rpi.edu
[3] Redfern Chair Professor and MOVE Director, AIAA Fellow, fgandhi@rpi.edu

an MBS software that employs both rigid and flexible elements to analyse nonlinear response of multi-body systems. Figure 1a shows the SIMPACK model for the quad-rotor wind turbine. It consists of four WindPact 1.5MW clock wise spinning rotors [15]. The blades, booms, and the tower are modelled as flexible bodies, whose deformations are represented as elastic modes. The remaining wind turbine components (nacelle, hub, yaw-bearings, etc..) are modelled as rigid bodies. Figure 1b shows the structural layout and dimensions of the tower-boom assembly for the quad-rotor wind turbine. The tower is 136.75m high with four 36.75m long booms attached in Double-T configuration with the top and bottom booms separated by 73.5m.

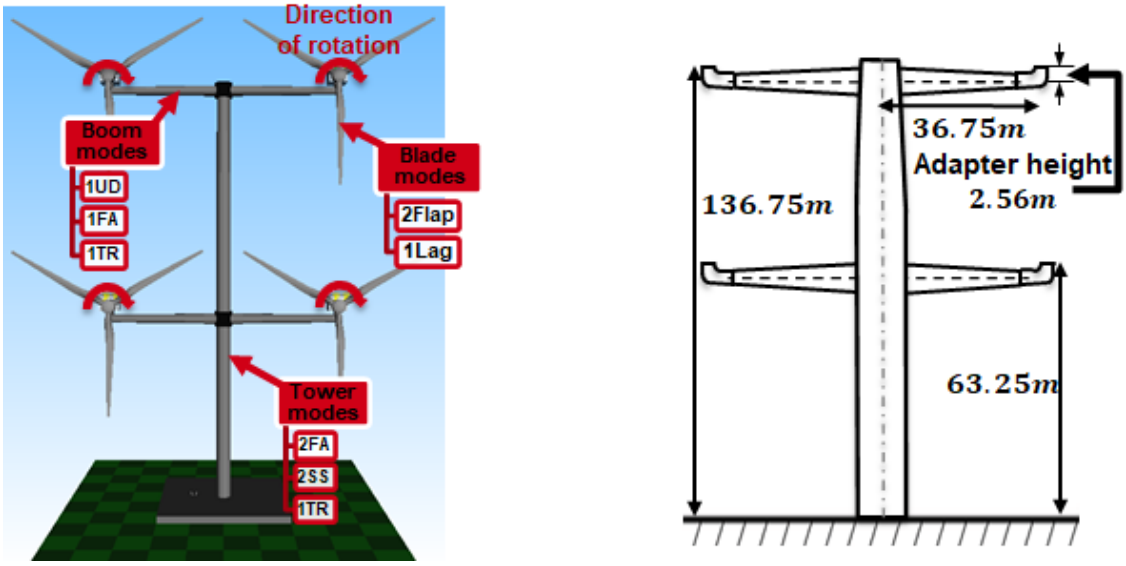

Fig. 1a: quad-rotor wind turbine model in SIMPACK. Fig. 1b: Dimensions of the Tower-Boom model

The tower is a hollow cylinder made of steel with Young's modulus of 2.1×10^{11} N/m^2 and mass density of 8100 kg/m^3. The bottom 70% of the tower consists of a constant outer diameter of 4.3m and tapers linearly to 3.7m at the tower top. The elastic deformation of the tower is modelled using mode shapes corresponding to the first two Fore-Aft (FA) and Side-Side (SS) modes together with the first Torsion (TR) mode.

Table 1.Gross Properties of Quad-Rotor wind turbine.

Parameters	Quad-Rotor	Single-Rotor
Rating	4×1.5MW	6MW
Control	Variable Speed, Collective Pitch	Variable Speed, Collective Pitch
Rotor, Hub Diameter	70m, 3.5m	140m, 7.0m
Hub Height	(top rotors)136.75m / (bottom rotors)63.25m	100m
Rated Wind Speed	11.4m/s	11.4m/s
Rated Rotor Speed	21.8rpm	10.9rpm
Rated Tip Speed	80 m/s	80 m/s
Overhang, Shaft Tilt, Precone	3.3m, 0°, 2.5°	5.5m, 0°, 2.5°

The upper portion of the tower of a GE 1.5MW turbine is used as the boom for the individual rotors of the quad-rotor turbine. The booms are $0.5(1+\delta_{sep})$D long, where D is the rotor diameter and δ_{sep} is the minimum rotor separation distance, set to 5% of rotor diameter in the current model [16]. The booms are of the same material as the tower and are modelled as linearly tapered cylinders with the maximum diameter of 3.4m realized at the intersection between the booms and the tower (see Figure 1b) and a minimum diameter of 2.6m. Furthermore, an adapter at the boom tip is attached to support the rotor-nacelle assembly. The elastic deformation of the booms is modelled using linear combination of the boom's first Fore-Aft (FA) and Up-Down (UD) mode shapes together with the first Torsion (TR) mode. The FA and UD mode shapes describe respectively the out-of-plane and in-plane deformation of the booms, with 'in-plane' defined as the plane containing the tower-boom assembly. The elastic deformation of the blades is modelled using linear combination of the first two flap modes and the first lag mode, with the blades assumed to be torsionally rigid. The foundation is modelled using clamped boundary condition. The salient properties of the quad-rotor wind turbine, together with a single-rotor with equivalent machine rating, are summarized in Table 1.

3. Aeroelastic stability analysis of Quad-Rotor wind turbines

The linearization of the wind turbine model is carried out at an equilibrium point for given operational parameters (e.g., mean wind speed, rotor speed) to capture the nonlinearities of the system. The current model considers quasi-steady rotor aerodynamics and as such the equation of motion for the quad-rotor wind turbine model may be written as:

$$\underline{\ddot{X}} = \underline{f}(\underline{\dot{X}}, \underline{X}, \underline{u}), \tag{1}$$

where the vector $\underline{u}$ represents the input vector that contains the operational parameters (wind speed, wind shear, tower shadow, etc…) and $\underline{X}$ is $N \times 1$ state vector containing degrees of freedom both in fixed and rotating frame, such that:

$$\mathrm{X} = \left\{ \mathrm{X_f} \quad \{\mathrm{q}_1^1 \quad \mathrm{q}_2^1 \quad \mathrm{q}_3^1 \quad \dots \quad \mathrm{q}_1^J \quad \mathrm{q}_2^J \quad \mathrm{q}_3^J\}_1 \quad \dots \quad \{\mathrm{q}_1^1 \quad \mathrm{q}_2^1 \quad \mathrm{q}_3^1 \quad \dots \quad \mathrm{q}_1^J \quad \mathrm{q}_2^J \quad \mathrm{q}_3^J\}_4 \right\}^{\mathrm{t}}, \tag{2}$$

where $\mathrm{X_f}$ is an $F \times 1$ vector representing the F degrees of freedom in the fixed frame. The degrees of freedom in the rotating frame are given by $\{\mathrm{q}^{\mathrm{i}}_{\mathrm{j}}\}_{\mathrm{b}}$ with subscript j denoting the three blades of rotor b (4 rotors in total) and superscript i referring to the i^{th} degrees of freedom of blade j, with the total number of degrees of freedom per blade denoted by J. The velocity and acceleration of the state vector are respectively given by $\underline{\dot{X}}$ and $\underline{\ddot{X}}$. The right-hand side in equation 1 contains the non-linear mass, stiffness, gyroscopic damping, and the quasi-steady aerodynamic forces (that depend on blade position and velocity) of the system.

Stability of the wind turbine model is evaluated by linearizing equation 1 around the steady-state point $(\underline{X}_0, \underline{\dot{X}}_0)$. The present work excludes the effect of wind shear and tower shadow and as such the only source of periodic load in the system is due to gravity which, in the case of identical blades, can be eliminated by employing MBC transformation to define all degrees of freedom in fixed frame. Furthermore, the linearization implemented in this paper is carried out in modal-space where perturbation of the state vector (at steady-state) is expressed in terms of a linear combination of mode-shapes, such that:

$$\left\{ \begin{matrix} \Delta\underline{X} \\ \Delta\underline{\dot{X}} \end{matrix} \right\}\Bigg|_{\underline{X}_0, \underline{\dot{X}}_0} = \begin{bmatrix} \mathbf{T} & \mathbf{0} \\ \Omega\partial\boldsymbol{T} & \mathbf{T} \end{bmatrix} \begin{bmatrix} \boldsymbol{\Phi} & \mathbf{0} \\ \mathbf{0} & \boldsymbol{\Phi} \end{bmatrix} \left\{ \begin{matrix} \underline{z} \\ \underline{\dot{z}} \end{matrix} \right\}, \tag{3}$$

Where Ω is the rotor speed, $\underline{z}$ is $M \times 1$ vector containing the degrees of freedom in modal space (modal coordinates), and $\boldsymbol{\Phi}$ is $N \times M$ matrix of mode-shapes, with N degrees of freedom of the model $(\underline{X})$ represented by M number of mode-shapes. Furthermore, $\mathbf{T}$ is a block diagonal matrix that maps degrees of freedom from fixed frame to rotating frame, while $\partial\boldsymbol{T}$ is the first derivative of $\mathbf{T}$ with respect to the rotor speed. Detailed description on implementing MBC transformation in the present framework is given in [12]. The mode-shapes are obtained from an eigenvalue analysis of the quad-rotor wind turbine without considering aerodynamic loads. Using equation 3, the nonlinear dynamics of a wind turbine model, given by equation 1, are numerically linearized using central finite difference scheme with the linearized model (in modal space) given by:

$$\left\{ \begin{matrix} \dot{\underline{z}} \\ \ddot{\underline{z}} \end{matrix} \right\} = \boldsymbol{A} \left\{ \begin{matrix} \underline{z} \\ \dot{\underline{z}} \end{matrix} \right\}, \tag{4}$$

where $\boldsymbol{A}$ is a linear time invariant system matrix of the wind turbine model at a given steady-state and operational point, taking the form:

$$\boldsymbol{A} = \begin{bmatrix} \mathbf{0}_{N\times M} & \boldsymbol{I}_{N\times M} \\ \boldsymbol{K}_z & \boldsymbol{C}_z \end{bmatrix}, \tag{5}$$

with the stiffness term (including both structural and aerodynamic stiffness) given by:

$$\boldsymbol{K}_z = \boldsymbol{\Phi}^{-1} \left(\boldsymbol{T}^{-1} \frac{\Delta \underline{f}}{\Delta \underline{z}}\Bigg|_{\underline{X}_0, \underline{\dot{X}}_0} - \Omega^2 \partial^2 \boldsymbol{T} \boldsymbol{\Phi} \right), \tag{6}$$

where $\partial^2\boldsymbol{T}$ is the second derivative of $\mathbf{T}$ with respect to the rotor speed. Likewise, the system's damping matrix (including both the gyroscopic and aerodynamic damping term) is given by:

$$\boldsymbol{C}_z = \boldsymbol{\Phi}^{-1}\left(\boldsymbol{T}^{-1}\frac{\Delta \underline{f}}{\Delta \underline{\dot{z}}}\Big|_{\underline{X}_0,\underline{\dot{X}}_0} - 2\Omega\partial\boldsymbol{T}\boldsymbol{\Phi}\right). \quad (7)$$

The standard eigenvalue analysis method can directly be used on the LTI system matrix (see equation 5) to extract the complex eigenvalues ($\boldsymbol{\lambda_n}$) and thereby evaluating the natural frequency and damping ratio of the quad-rotor wind turbine model; with the natural frequency and damping ratio given, respectively, by:

$$\omega_n = \frac{\boldsymbol{Im}\{\lambda_n\}}{2\pi}, \quad (8)$$

and

$$\xi_n = -\frac{\boldsymbol{Re}\{\lambda_n\}}{|\lambda_n|}. \quad (9)$$

In order to determine the stability of a quad-rotor wind turbine, it is required to linearize the wind turbine model at different wind speeds between cut-in and cut-out. During the linearization of the model (at a given wind speed), the blade pitch angle and rotor speed are fixed. Therefore, the steady-state power, blade pitch angle and rotor speed of a quad-rotor wind turbine as a function of wind speed, shown in Fig. 2, is employed during the linearization process. The vertical axis on the left side of Fig.2 shows the rotor speed (RPM) and blade pitch angle (deg), while the right vertical axis presents the generated power (MW) for a WindPact 1.5MW rotor. Furthermore, Fig. 2 shows that, before the rated wind speed, the turbine is generator controlled (variable rotor speed) and pitch controlled after rated wind speed (constant rotor speed).

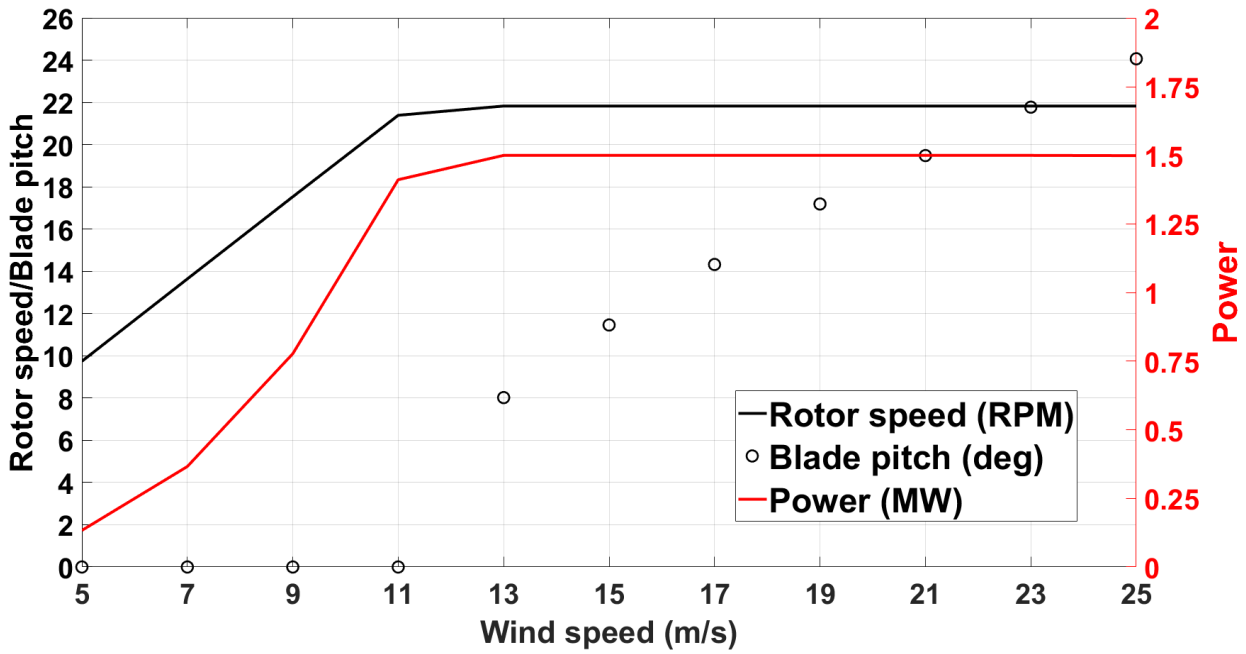

Figure 2. Power, pitch and rotor speed as a function of wind speed for WindPact 1.5MW rotor.

Finally, a mode comparison method is used to determine how the individual modes vary with changing wind speed. Mode clustering by ordering (from low to high) the natural frequencies for different wind speeds is not effective since the natural frequency of some modes tend to cross each other with changing wind speeds. An effective method for mode clustering (MACXP), proposed by [18], is employed here since it is proven to be effective in mode clustering of aeroelastic systems [11,19].

4. Verification of the proposed method

The linearization method described earlier is verified by comparing the frequency and damping ratios of the NREL 5MW machine with results from [6]. Details of the NREL 5MW model used for aeroelastic stability analysis is given in [6]. Figure 3 shows the damping ratio versus inflow wind speed of the NREL 5MW machine, with the solid lines obtained using the present formulation and the dashed lines from [6]. The damping ratios are divided into two categories: low damping (< 10%) and high damping (>30%).

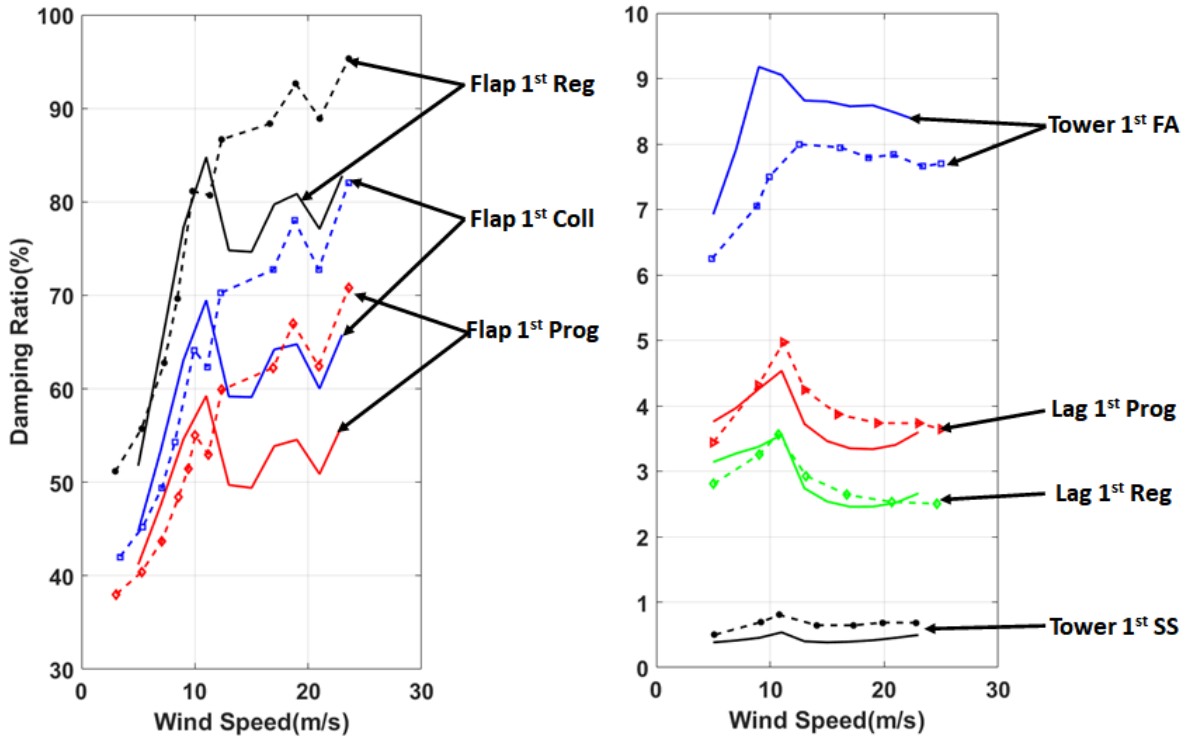

Figure 3. Comparison of damping ratio for NREL 5MW machine. The solid lines are obtained using the present formulation and the dashed lines are from [6].

Figure 3 shows that the present method is able to capture fairly well the trend in the damping ratios giving good confidence that the proposed method is appropriate in analysing the aeroelastic stability of a quad-rotor wind turbine. Particularly, the low damping results from the present methods match quite will with the results from [6] and with the proposed method yielding an overall conservative damping ratio result compared to [6]. The frequency results have also been verified and compare well with frequency results from [6] (results not included in the paper).

5. Quad-Rotor Wind Turbine Aeroelastic Stability

Stability analysis of a wind turbine starts first with modal analysis of the system spinning in vacuum; since the modal frequencies together with the associated mode-shapes provide insight into the system's dynamics and help identify dominant modes. The non-linear time varying dynamic model of the model is linearized at various hub-height wind speeds ranging between 5m/s and 25 m/s with an increment of 2m/s; representing the cut-in and cut-out wind speeds of the WindPact 1.5MW machines mounted on the quad-rotor support structure shown in Fig. 1. The wind turbine model is linearized at each wind speed using the operational points given in Fig. 2 and considering gravity while neglecting wind shear and tower shadow.

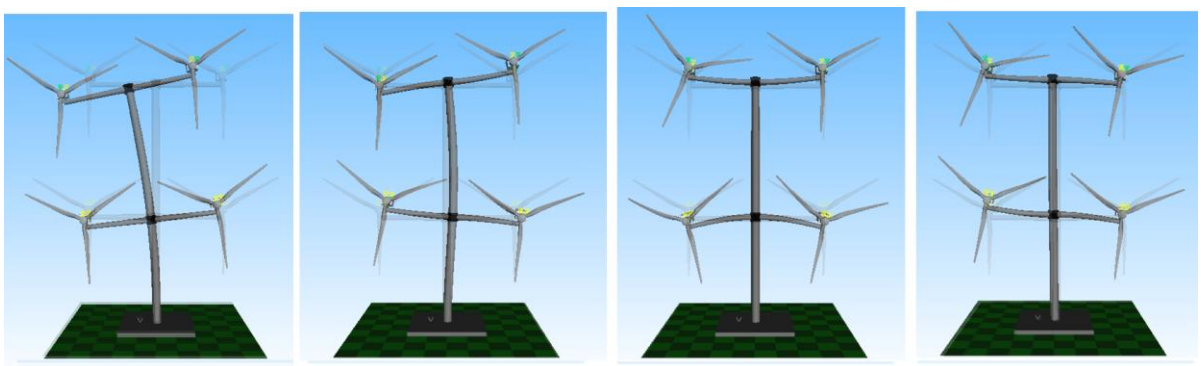

Figure 4. Mode-shapes corresponding to the natural frequency curves shown with black lines in Fig. 6. From left to right: Tower 1st SS, Tower 2nd SS, Boom Coll UD, Boom Diff UD

Figure 5 shows the natural frequency (left) and damping ratio (right) of a quad-rotor wind turbine as a function of wind speed, with each rotor corresponding to that on the WindPact 1.5MW turbine. The different modes shown in Fig. 5 are colour coded such that: the modes given by different shades of black correspond to modes-shapes comprised solely of support-structure (tower and booms) constrained to in-plane motion (in-plane implying rotor plane) as shown in Fig. 4; the modes given by different shades of blue correspond to mode-shapes comprised solely of support-structure (tower and booms) constrained to out-of-plane motion as shown in Fig. 6; the modes given by different shades of green correspond to mode-shapes consisting of a combination of boom and rotor modes; the modes given by different shades of red correspond to mode-shapes consisting solely of rotor modes. Stability results for modes shaped with higher natural frequency are omitted from analysis as these mode-shapes are unlikely to be excited by aerodynamic load and there is no indication of any self-excitation in the system. Particularly, the rotor lag modes (collective, regressive and progressive) all have high natural frequency that they do not interact with the dominant rotor excitation frequencies (1P and 3P) in addition of being sufficiently well damped. Furthermore, Fig. 6 shows in dashed line the 1P and 3P excitation frequency as a function of wind speed; with the 1P and 3P excitation frequency increasing linearly with wind speed until rated speed and remain constant after rated wind speed (following pitch regulated wind turbine control strategy).

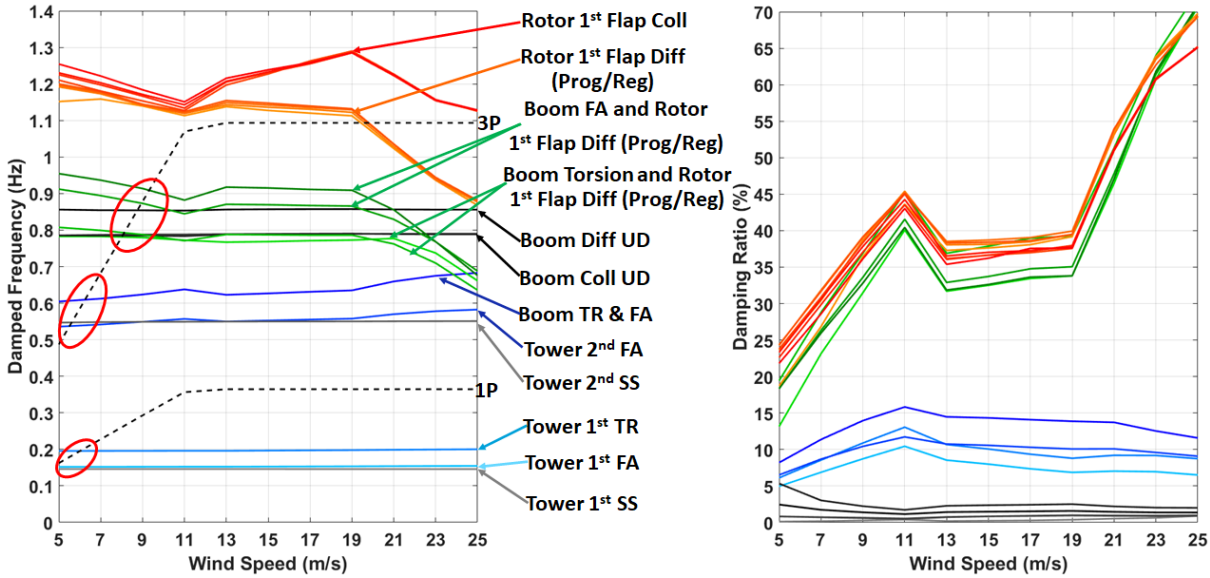

Figure 5. Variation of damped natural frequencies and damping ratios with mean wind speed for mode shapes that include tower side-side mode.

Looking at Fig. 5, the modes comprised of purely rotor modes (red curves) are highly damped, with damping ratio ranging between 10-70%. Furthermore, the natural frequency curves of the modes shown in red tends to change with wind speed due to mainly of centrifugal stiffening. Particularly, the natural frequency decreases roughly linearly for wind speeds less than the rated speed and diverge into two opposing curves at rated wind speed. Additionally, after 19m/s, the natural frequency of all rotor modes tends to exhibit similar gradient in the frequency curve. The sudden change in natural frequency at the rated wind speed is due to change in control strategy: from generator controlled to pitch controlled power regulation. similarly, the damping ratio of these modes seems to vary linearly up to rated speed, drop slightly and remain constant up to 19m/s and increase roughly linearly afterwards. Similarly, the modes comprised of a combination boom fore-aft and rotor flap modes (shown in green) also show high damping, with damping ratio in 10-70% range. Furthermore, Fig. 5 shows that the 3P excitation, which is the dominant aerodynamic excitation to the support structure (tower and booms), intersects several natural frequency curves of the system (dashed lines circled in red).

The mode-shapes confined to in-plane motion (see Fig. 4) may be of concern as they have low damping (see left window in Fig. 5). This is further examined in Fig. 7 where the natural frequency and damping ratio of the mode-shapes shown in Fig. 4 are isolated. Additionally, the dashed line in Fig. 7 represents the natural frequency and damping of an equivalent 6MW single-rotor wind turbine's 1st tower side-side mode. Figure 7 shows that three modes (Tower 1st SS, Tower 2nd SS, Boom Coll UD) are identified with low damping where the damping ratio is less than 1% over the entire operation range and the Boom Diff UD mode (see Fig. 4) is slightly more damped, with the damping ratio between 1-2.5% below rated and in the 1-1.5% range after rated speed. Furthermore, Fig.

7 shows that the natural frequencies of these modes do not change with wind speed while the trend in the damping ratio changing abruptly after the rated wind speed. This change in damping ratio is due to change in turbine operation; where, before rated speed, the power is regulated by the generator torque and blade pitch after rated wind speed (see Fig. 2). Additionally, the trend in damping ratio of the 2nd side-side tower and collective up-down booms (see Fig. 7) seem to follow closely one another. Finally, the pre-rated trend in damping ratio of the 1st side-side tower mode in seen to be opposite to the remaining modes shown in Fig. 7, with the damping ratio of remaining three modes decreasing with increasing wind speed.

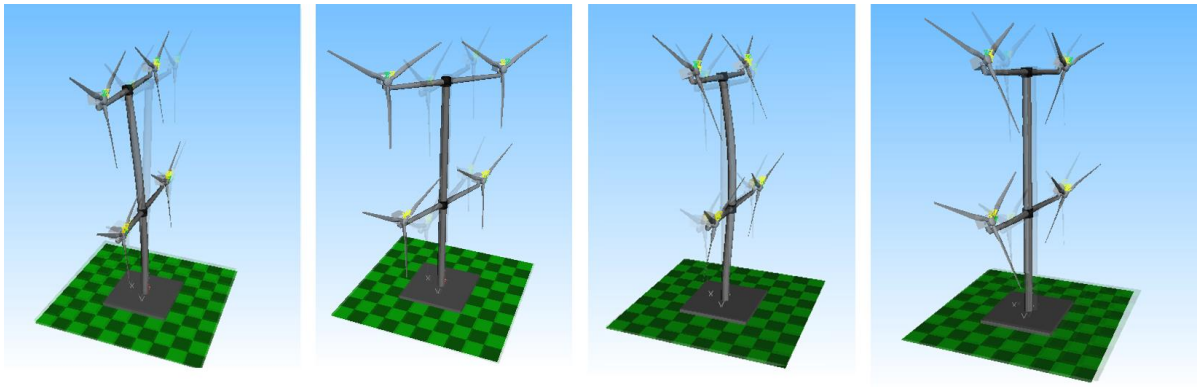

Figure 6. Mode-shapes corresponding to the natural frequency curves shown with blue lines in Fig. 6. From left to right: Tower 1st FA, Tower 1st TR, Tower 2nd FA, Boom TR & FA

Fig. 7 also shows that the quad-rotor 1st side-side tower mode is slightly more damped than the single rotor counterpart. Moreover, the results seem to indicate that the post rated damping of the 1st tower side-side mode of the quad-rotor wind turbine seems to increase more with wind speed than for the single-rotor counterpart.

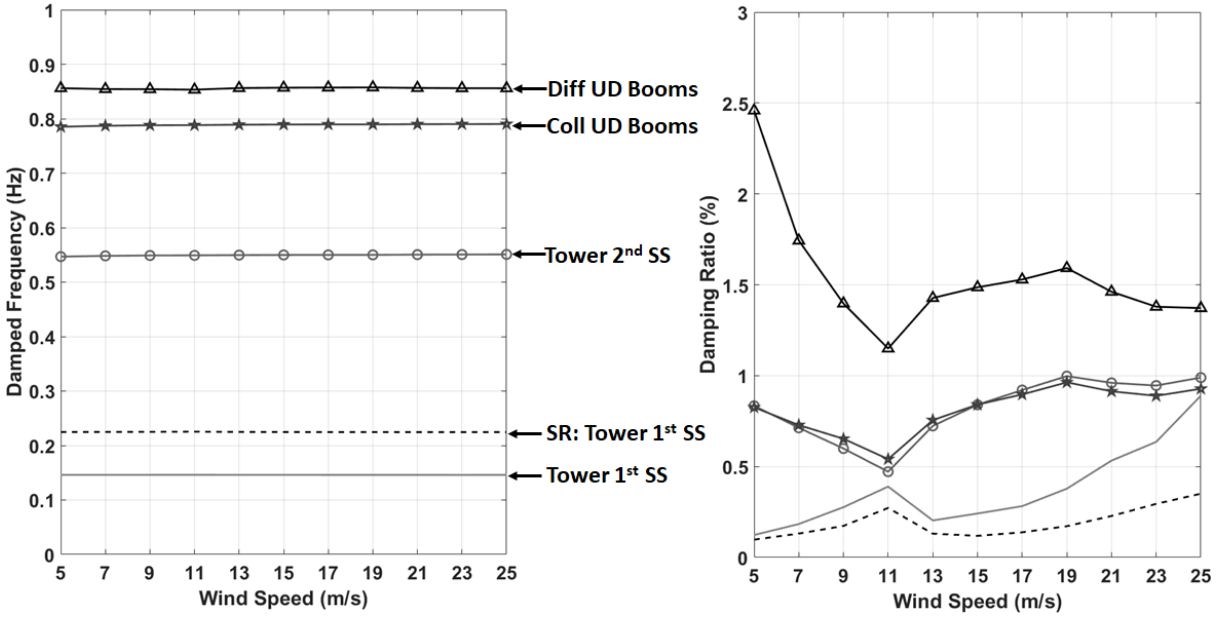

Figure 7. Variation of damped natural frequencies and damping ratios with mean wind speed for mode shapes that include tower fore-aft mode.

After the lowest damped modes shown in Fig. 7, the tower 1st and 2nd fore-aft, 1st torsion and combination of boom torsion & fore-aft modes are seen to be well damped. This is shown in Fig. 8, where the natural frequency and damping ratio of mode-shapes consisting of out-of-plane tower and boom modes (see Fig. 6) are shown separately. Furthermore, the dashed line in Fig. 8 represents the 1st fore-aft tower mode of the single-rotor wind turbine with equivalent machine rating (see Table 1 for the salient properties). These are seen to be well damped, with the critical damping ratio generally varying between 6-15% across the operational range. The natural frequencies of the 1st fore-aft and torsion tower modes do not change with wind speed. However, the 2nd fore-aft tower mode and the boom torsion & fore-aft mode vary slightly with wind speed, most likely due to gyroscopic effect. The damping

ratio for the 1st fore-aft tower mode is lower for the quad-rotor wind turbine compared to the single-rotor counterpart. This is most likely due to the larger aerodynamic damping relative to the rotor plus tower inertia for the single-rotor machine compared to the quad-rotor wind turbine. Furthermore, the corresponding damping (see the right window in Fig. 8) shows a linear increase in the damping ratio with wind speed up to the rated speed then continually drops in the post rated region, following the same thrust vs wind speed trend in pitch-controlled wind turbines. The damping ratio of the 1st torsion and 2nd fore-aft tower modes follow similar trend, especially for before rated wind speeds.

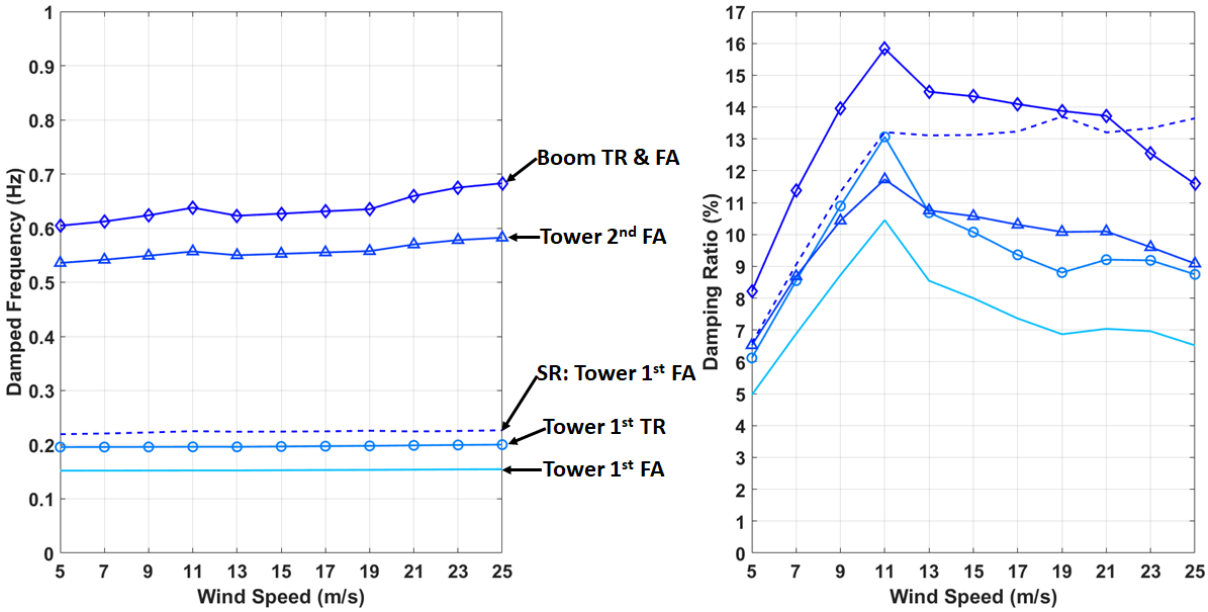

Figure 8. Variation of damped natural frequencies and damping ratios with mean wind speed for mode shapes that include tower fore-aft mode.

For the quad-rotor wind turbine, the total damping has contribution both from the top and bottom rotors. Figure 9 shows the breakup of the top and bottom rotor contributions to damping in the 1st & 2nd fore-aft and 1st torsion mode. In Fig. 9, the red bars represent the case where all the rotors are active, i.e., generate aerodynamic load. The green bars represent active top rotors only, and the blue bars represent active bottom rotors only. It is evident from the figure that, in the case of 1st fore-aft and 1st torsion tower modes, the dominant contributor to aerodynamic damping are the top rotors, while the bottom rotors contribute mostly to the aerodynamic damping in the case of the 2nd fore-aft tower mode. This is to be expected since the bottom rotors have the highest fore-aft velocity when the quad-rotor support structure is exited in the 2nd fore-aft mode resulting in higher aerodynamic damping. Lastly, although the natural frequencies of the modes in Fig. 9 are excited by the 1P and 3P blade passing frequency (see Fig. 6), this is not a matter of concern since these modes are sufficiently damped.

6. Conclusions

This paper presents the aeroelastic stability analysis of a quad-rotor wind turbine (comprised of 4 rotors arranged in double T-format on a single tower) and identifies the damped natural frequencies and the corresponding damping ratios. First, an aeroelastic analysis of the wind turbine model for a range mean wind speeds excluding atmospheric boundary layer and tower shadow is run until a quasi-steady state is reached; followed by the linearization of the plant around the steady-state resulting in linear time periodic system. MBC transformation is applied to write the states in the fixed frame resulting in linear time invariant system followed by standard eigenvalue analysis to determine the natural frequency and damping ratio of the quad-rotor wind turbine for a range of wind speeds between cut-in and cut-out. The resulting natural frequency and damping ratio of the system are analysed in detail and the following conclusions on the stability of a quad-rotor wind turbine are reached:

- Several support structure (tower and booms) dominated modes (Tower 1st side-side, Tower 2nd side-side, Boom collective up-down) are identified with low damping where the damping ratio is less than 1% over the entire operation range and the next support structure mode which is slightly more damped is the boom differential up-down mode, with the damping ratio between 1-2.5% below rated and in the 1-1.5% range after rated speed.

- The 3P excitation, which is the dominant aerodynamic excitation load of the support structure, intersects with several modes of the wind turbine. Particularly, the mode-shapes confined to in-plane motion (Tower 1st side-side, Tower 2nd side-side, Boom collective up-down) may be of concern as they have low damping (less than 1%).
- Following the lowest damped modes, the tower 1st and 2nd fore-aft, 1st torsion and combination of boom torsion and fore-aft modes are seen to be well damped, with the critical damping ratio generally varying between 6-15% across the operational range.
- For the quad-rotor wind turbine, the total damping has contribution both from the top and bottom rotors, where in the case of the 2nd fore-aft tower mode, the bottom rotors are the dominant contributors while the top rotors are dominant contributors for the damping of the 1st fore-aft and 1st torsion tower modes. This is to be expected since the bottom rotors have the largest fore-aft velocity when the quad-rotor support structure is excited in 2nd fore-aft mode resulting in higher aerodynamic damping.
- The modes comprised of purely rotor modes are highly damped, with damping ratio in 10-70% range. Similarly, the modes comprised of boom fore-aft and rotor flap modes also show high damping, with damping ratio in 10-70% range.

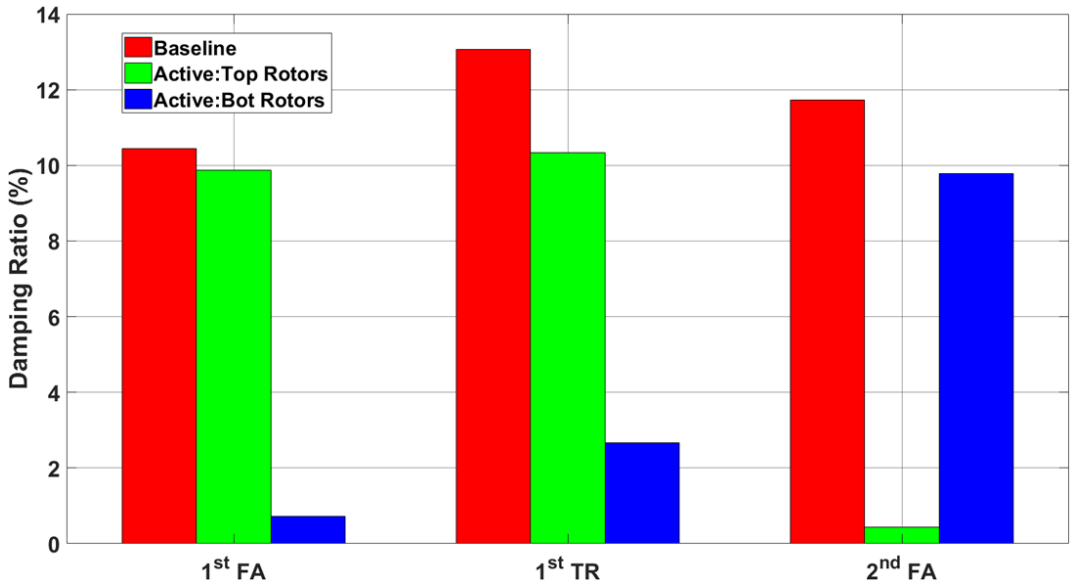

Figure 9. Sensitivity of damping ratio of select tower modes as a function of the active (aerodynamic) rotors.

Acknowledgments

This study was funded by the New York State Energy Research and Development Authority (NYSERDA) and General Electric (GE) Renewables under Award No.127346, Quad-Rotor Wind Turbine, with Mr. Richard Bourgeois (NYSERDA) and Mr. Peter Maxwell (GE) as the Program Managers. Their support is gratefully acknowledged. NYSERDA and GE have not reviewed the information contained herein, and the opinions expressed in this report do not necessarily reflect those of NYSERDA or GE.

References

[1] Hansen, M. O. L., Sørensen, J. N., Voutsinas, S., Sørensen, N., & Madsen, H. A. (2006). State of the art in wind turbine aerodynamics and aeroelasticity. *Progress in aerospace sciences*, *42*(4), 285-330.

[2] Murtagh, P. J., & Basu, B. (2007). Identification of equivalent modal damping for a wind turbine at standstill using Fourier and wavelet analysis. *Proceedings of the Institution of Mechanical Engineers, Part K: Journal of Multi-body Dynamics*, *221*(4), 577-589.

[3] Rezaeian, A. AEROELASTIC STABILITY ANALYSIS OF WIND TURBINES CONSIDERING THE INSTABILITIES KNOWN FROM ROTARY WING DYNAMICS. International Forum on Aeroelasticity and Structural Dynamics(IFASD), 2019.

[4] Riziotis, V. A., Voutsinas, S. G., Politis, E. S., & Chaviaropoulos, P. K. (2004). Aeroelastic stability of wind turbines: the problem, the methods and the issues. *Wind Energy: An International Journal for Progress and Applications in Wind Power Conversion Technology*, *7*(4), 373-392.

[5] Bir, G., "Multi-blade coordinate transformation and its application to wind turbine analysis," *46th AIAA aerospace sciences meeting and exhibit*, 2008, p. 1300.

[6] Bir, G., & Jonkman, J. (2007, July). Aeroelastic instabilities of large offshore and onshore wind turbines. In *Journal of Physics: Conference Series* (Vol. 75, No. 1, p. 012069). IOP Publishing.

[7] Skjoldan, P. F., & Hansen, M. H. (2009). On the similarity of the Coleman and Lyapunov–Floquet transformations for modal analysis of bladed rotor structures. *Journal of Sound and Vibration*, *327*(3-5), 424-439.

[8] Riva, R., Cacciola, S., & Bottasso, C. L. (2016). Periodic stability analysis of wind turbines operating in turbulent wind conditions. *Wind Energy Science*, *1*(2), 177-203.

[9] Bottasso, C. L., & Cacciola, S. (2015). Model-independent periodic stability analysis of wind turbines. *Wind Energy*, *18*(5), 865-887.

[10] Filsoof, O. T., Hansen, M. H., Yde, A., Bøttcher, P., & Zhang, X. (2021). A novel methodology for analyzing modal dynamics of multi-rotor wind turbines. *Journal of Sound and Vibration*, *493*, 115810.

[11] Filsoof, O. T., Yde, A., Bøttcher, P., & Zhang, X. (2021). On critical aeroelastic modes of a tri-rotor wind turbine. *International Journal of Mechanical Sciences*, *204*, 106525.

[12] Ferede, E., & Gandhi, F. (2020, September). Modal analysis of a quad-rotor wind turbine. In *Journal of Physics: Conference Series* (Vol. 1618, No. 3, p. 032002). IOP Publishing.

[13] Coleman, R. P., & Feingold, A. M. (1958). *Theory of self-excited mechanical oscillations of helicopter rotors with hinged blades* (pp. 269-307). US Government Printing Office.

[14] Rulka, W., "SIMPACK—A computer program for simulation of large-motion multibody systems," *Multibody systems handbook*, Springer, 1990, pp. 265–284.

[15] Jonkman, J., Hayman, G., Jonkman, B., Damiani, R., and Murray, R., "AeroDyn v15 User's Guide and Theory Manual," *NREL: Golden, CO, USA*, 2015.

[16] Van der Laan, P., Andersen, S. J., García, N. R., Angelou, N., Pirrung, G., Ott, S., Sjöholm, M., Sørensen, K. H., Neto, J. X. V., Kelly, M. C., et al., "Power curve and wake analyses of the Vestas Multi-Rotor demonstrator," *Wind Energy Science*, Vol. 4, No. 2, 2019, pp. 251-271.

[17] van der Laan, M. P., and Abkar, M., "Improved energy production of Multi-Rotor wind farms," *Journal of Physics: Conference Series*, Vol. 1256, IOP Publishing, 2019, p. 012011.

[18] Vacher, P., Jacquier, B., & Bucharles, A. (2010, September). Extensions of the MAC criterion to complex modes. In *Proceedings of the international conference on noise and vibration engineering* (pp. 2713-2726).

[19] Schwochow J, Jelicic G, SchwochowJ and Jelicic G. Automatic Operational Modal Analysis for Aeroelastic Applications. In: 6th International opera- tional modal analysis conference; 2015. p. 12 —-14. ISBN 9788578110796. doi: 10.1017/CBO9781107415324.004.